Anomalously High Thermal Conductivity of Amorphous Silicon Films Prepared by Hot-wire Chemical Vapor Deposition

Xiao Liu,[1,*] J. L. Feldman,[1,2] D. G. Cahill,[3] Ho-Soon Yang,[4] R. S. Crandall,[5] N. Bernstein,[1] D. M. Photiadis,[1] M. J. Mehl,[1] and D. A. Papaconstantopoulos[1,2]

[1]*Naval Research Laboratory, Washington, D. C. 20375, USA*
[2]*Department of Computation and Data Sciences, George Mason University, Fairfax, Virginia, 22030, USA*
[3]*Department of Materials Science and Engineering, and Material Research Laboratory, University of Illinois, Urbana, Illinois 61801, USA*
[4]*Department of Physics, Pusan National University, Pusan 609-735, Korea*
[5]*National Renewable Energy Laboratory, Golden, Colorado 80401, USA*

(Received March 11, 2010)

We report anomalously high thermal conductivities of amorphous Si (a-Si) films prepared by hot-wire chemical-vapor deposition (HWCVD) at the National Renewable Energy laboratory (NREL), that is a factor of 4∼6 higher than predicted by the model of minimum thermal conductivity. The temperature dependent thermal conductivities are measured with the time-domain thermoreflectance method on two thin films and with the $3\,\omega$ method on a thick film. For all these films, the thermal conductivity shows a strong phonon mean free path dependence that has so far only been found in crystalline semiconductor alloys. Similar HWCVD a-Si films prepared at the U. Illinois do not show an enhanced thermal conductivity even though the Raman spectra of the NREL and the U. Illinois samples are essentially identical. We also applied a Kubo based theory using a tight-binding method on three 1000 atom continuous random network models. The theory gives higher thermal conductivity for more ordered models, but not high enough to explain our results, even after extrapolating to lower frequencies with a Boltzmann approach. Our results show that the thermal conductivity of a-Si depends strongly on the details of their microstructure that are not revealed by vibrational spectroscopy.

PACS numbers: 65.60.+a, 63.50.-x, 66.70.-f

I. INTRODUCTION

The nature of heat transport in disordered solids is still poorly understood. At low temperatures, the T^2 dependent thermal conductivity (κ) below 1 K is understood as caused by phonon scattering of the atomic tunneling states (TS), common in amorphous solids but unknown in origin [1]. The high temperature features, such as the plateau at near 10 K, the continued rise of κ with T at above 40 K, and the near saturation at higher T are still debated as well [2–7], where the model of minimum thermal conductivity [4, 5], the fracton theory [6], and a Kubo based theory [7] have all been applied to the high temperature regime.

In this work, we report on temperature and laser-modulation-frequency dependent

measurements of κ of two thin ($\sim$2 μm) and one thick (80 μm) hydrogenated amorphous silicon (a-Si) films with 1 at.% H prepared by hot-wire chemical-vapor deposition (HWCVD) at the National Renewable Energy laboratory (NREL). This type of a-Si prepared at the NREL has shown a range of novel properties, including the lack of the two-level tunneling states [8] that are characteristic of nearly all other amorphous solids. We show that its thermal conductivity is about a factor of 4–6 higher than predicted by the model of the minimum thermal conductivity. We also show a strong phonon mean free path (`l`) dependence with `l` up to 612 nm still contributing to the thermal conductivity, in conflict with the model of minimum thermal conductivity. In contrast, similarly HWCVD a-Si films prepared at the U. Illinois do not show an enhanced thermal conductivity even though the Raman spectra of the U. Illinois and the NREL samples are essentially identical. To explain the results, we have performed Kubo based calculations using a tight-binding electronic structure method and examined three different continuous random network (CRN) based models of a-Si [9]. We find that the theory gives higher κ for more structurally ordered models within the wavelength limit of their finite size, but not high enough to explain the high κ in the NREL a-Si films, even after extrapolating to lower frequencies with a Boltzmann approach.

II. EXPERIMENT

Three HWCVD a-Si films prepared at the NREL were studied in this work. They were deposited at a substrate temperature of 425 °C with the SiH_4 flow rate of 20 sccm, on crystalline Si substrates for two thin films (H14, 1.6 μm; H35, 2.8 μm) and on a stainless steel substrate for a thick film (H84, 80 μm). Growth rates were 0.8 nm/s for H14, 1.0 nm/s for H35 and 2.8 nm/s for H84. For H84, deposition was lasted for 8 hours to achieve the desired thickness to perform standard $3\,\omega$ measurement. As a result, some annealing may have taken place and its surface was then polished to remove hydrogen bubbles. The low temperature internal friction of H14 and H35 was published in ref. [8], where the disappearance of the two-level tunneling states was reported. In the same paper, a similarly prepared 2 μm thick film was characterized to be fully amorphous by high resolution TEM and electron diffraction. In this work, Raman measurements on all these three films again showed their Raman spectra were the same as a typical a-Si.

A second set of HWCVD a-Si films were prepared at the U. of Illinois on sapphire substrates at substrate temperatures between 114 and 600 °C to explore how the Raman spectra and thermal conductivity vary with deposition temperature. The growth rate of the U. Illinois samples was 0.3 nm/s, and film thicknesses were about 180 nm for this set of films.

To add to the discussion and further validate the experiments, we also studied the thermal conductivity of a 500 nm thick layer of a-SiO_2 formed by thermal oxidation of a silicon wafer and a bulk substrate of 8 $\omega\,t$.% yttria-stabilzed zirconia (YSZ). YSZ is a disordered crystalline oxide with a glass-like thermal conductivity.

Thermal conductivities were measured mostly by the time-domain thermoreflectance (TDTR) method [10], except for the temperature dependent thermal conductivity of H84

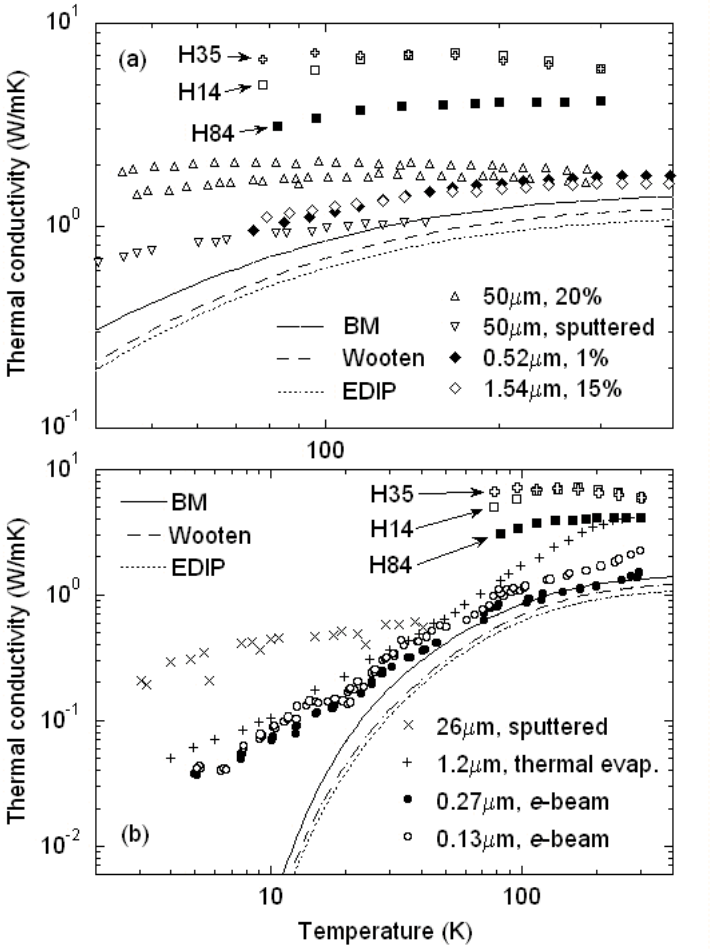

FIG. 1: κ of a-Si vs T. Our results are compared with previous ones: (a) above 40 K, (b) down to 2 K. The 50 μm data are from Ref. [11]; the 26 μm, Ref. [12]; the 0.52 and 1.45 μm, Ref. [13]; the 1.2 μm, Ref. [14]; the 0.13 and 0.27 μm, Ref. [15]. The Kubo based theory results for the three CRNs as detailed later in the text are represented by the lines labeled.

where standard 3ω method [11] were used.

III. RESULTS

The thermal conductivity results of the three HWCVD a-Si films prepared at the NREL are shown in Figure 1, together with most of the temperature dependent results available in literature so far. H14 and H35 were measured with the TDTR method at 1.1 MHz. H84 was measured with the standard 3ω method. Figure 1(a) focuses on measurements above 40 K, while Figure 1(b) shows four more measurements that extend to below

10K. We note that a-Si can have different microstructures depending on film preparation, hydrogenation, and heat treatment that may all impact κ. If boundary scattering dominates, κ could also show a film thickness dependence. The variation of κ in a-Si may have been further complicated by the difficulties of measuring κ of thin films. While most of the κ in Figure 1 show values between 1 and 2.5 W/mK near 300 K [11–15], room temperature only measurements show a wider variation, to as high as $4 \sim 6$ W/mK in a few indirect measurements based on diffusivity [16] (not shown). Over the entire temperature range covered, our result is significantly higher than any of the previous ones, and they are about $4 \sim 6$ times higher than predicted by the model of minimum thermal conductivity. The thermal conductivities of H14 and H35 are higher than that of H84, probably due to the optimized growth condition for these two thin films mentioned earlier. In addition, the thermal conductivities of H14 and H35 reach a maximum near 150 K. Both the magnitude and temperature dependence of the thermal conductivities are more reminiscent of semiconductor alloys [17] than typical amorphous solids such as a-SiO_2.

The three NREL films not only show anomalously high values of thermal conductivity, but also show a strong modulation frequency dependence of the pump laser beam used in the TDTR experiments shown in Figure 2. The thermal conductivity measured at 9.8 MHz modulation frequency is nearly a factor of 2 smaller than the conductivity measured at 1.1 MHz at all temperatures. Results of H14 and H35 are similar. We only show H14 at 115K and at room temperature in Figure 2. H84 is only measured at room temperature and the results are shown. In the limit of low modulation frequency, our $3\,\omega$ and TDTR results on H84 agree within 10%. In a TDTR experiment, phonons with $\mathtt{l}$ longer than the spatial extent of the T gradient do not contribute to the measured value of κ [10]. The agreement between the $3\,\omega$ and the TDTR measurements at 1.11 MHz suggests that phonons with $\mathtt{l} > (D/\omega)^{1/2} = 612$ nm are not significant for thermal conduction in this sample. Furthermore, the difference between the high and low frequency measurements by TDTR indicates that phonons with 162 nm $< \mathtt{l} <$ 612 nm contribute $\sim 40\%$ of κ of the sample. For comparison, a-SiO_2 and YSZ do not show a significant frequency dependence larger than the uncertainties in the measurements, also shown Figure 2. The frequency dependence and the magnitude of the room temperature data for a-Si in Figure 2 are almost identical to what we observed previously in crystalline SiGe alloys [10].

However, we could not duplicate the anomalously high thermal conductivity of the NREL HWCVD a-Si in films similarly prepared at the U. of Illinois. Figure 3 shows how the room temperature thermal conductivity varies with the substrate temperatures during deposition of the U. Illinois samples. The thermal conductivity increases with deposition temperature but only exceeds 2 W/mK at the highest deposition temperature. The a-Si films prepared at the U. Illinois are relatively thin, $\sim$180 nm in thickness; therefore, we could not reliably measure their thermal conductivity at low modulation frequencies. At 9.8 MHz, however, the thermal penetration depth is smaller than the film thickness, $(D/\omega)^{1/2} = 170$ nm, and we do not expect that the smaller film thickness of the U. Illinois could make a meaningful difference in the results. The room temperature thermal conductivity of the three NREL a-Si films measured at 9.8 MHz are included in Figure 3 for comparison.

All the a-Si films studied in this work are further characterized by Raman spec-

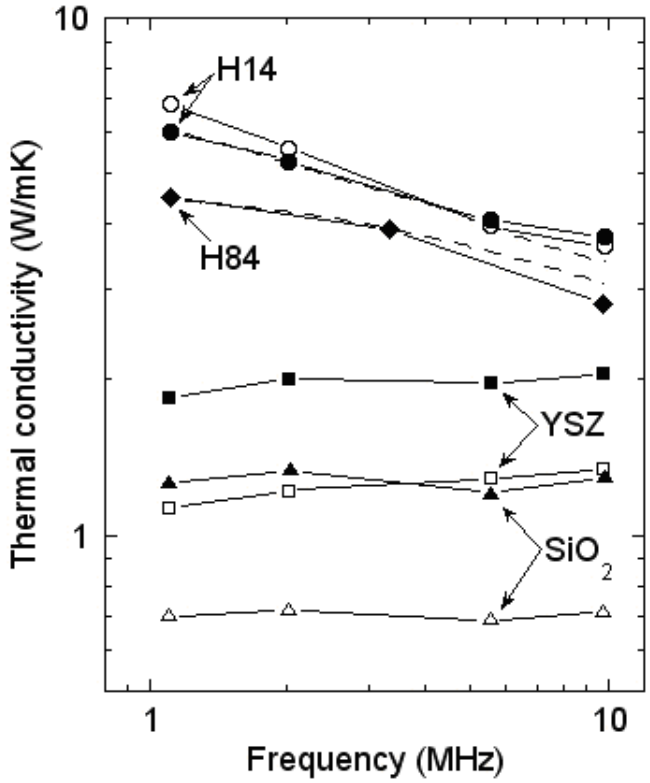

FIG. 2: Thermal conductivity of the NREL prepared a-Si (H14 and H84), YSZ, and SiO_2 as a function of the modulation frequency used in the TDTR measurements. The open symbols are for data taken at $T = 115$ K and filled symbols are for room temperature, except for YSZ where open symbols are for data taken at 154 K and filled symbols are for 328 K. The dashed lines show theoretical estimates of the frequency dependence explained later in the text.

troscopy, although the NREL a-Si samples have been extensively characterized and we have little doubt that the samples are truly amorphous. Figure 4 compares the Raman spectra of the NREL samples H14 (grown at 425 °C) with that of the U. Illinois a-Si sample grown at 400 °C. (Raman spectra of samples of H14 and H35 are indistinguishable.) The spectra of both the NREL and U. Illinois samples are almost identical and they are typical of a-Si. The main difference between the two, however, is the presence of the 615 cm^{-1} peak in the U. Illinois sample. Since the broad peak near 615 cm^{-1} is commonly associated with "wagging" vibrations of Si-H bonds [18], this suggests that growth conditions at the U. Illinois produce, for unknown reasons, higher hydrogen content. Raman spectra also show a consecutive reduction of the 615 cm^{-1} peak in the U. Illinois samples with increasing the deposition temperature (not shown), although they are all amorphous even at the highest deposition temperature. A change of hydrogen content may explain the

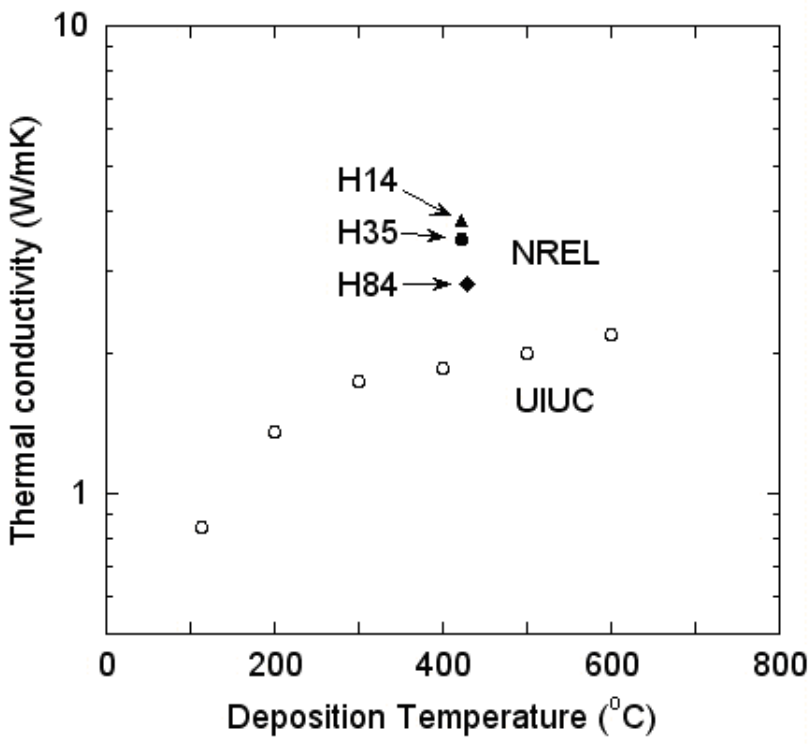

FIG. 3: Room temperature thermal conductivities of HWCVD a-Si films prepared at the U. Illinois as a function of the substrate temperature during deposition. The NREL results are shown for comparison. All results shown here are taken by the TDTR experiments at the modulation frequency of 9.8 MHz.

thermal conductivity variation in the U. Illinois a-Si films shown in Figure 3. But it still can not explain the anomalously high thermal conductivity in the NREL films.

IV. DISCUSSION

To understand the high thermal conductivity, we apply Kubo based theory in the harmonic approximation to compute the vibrational spectrum using a TB electronic structure total energy method [19] with the parameters derived from Ref. [20]]. Anharmonicity has been shown to have a small effect on κ [21]. We use three 1000 atom CRNs which differ in structural ordering (see Ref. [9] and references therein) and are all "relaxed" within our TB method. The Wooten model is based on an initial diamond structure and a bond switching algorithm, the Barkema and Mousseau (BM) model uses a generated random distribution as an initial configuration, and the environment dependent interatomic potential (EDIP) model is based entirely on a molecular dynamics quench from the liquid.

The acoustic projected spectral density $S(Q, E)$ is shown in Figure 5. Our results

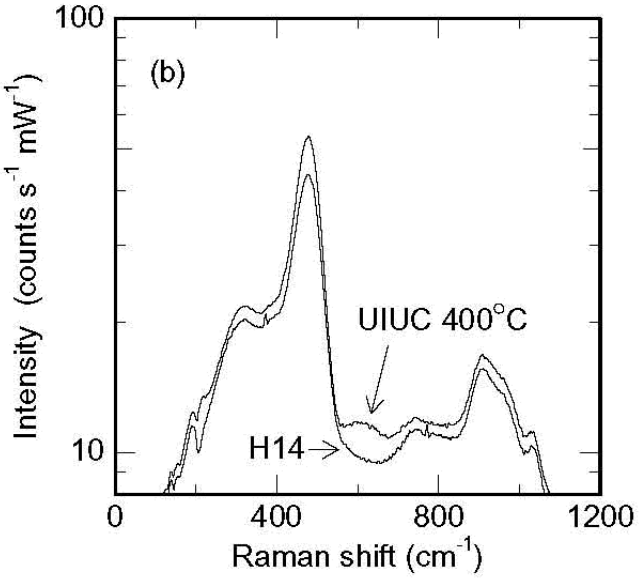

FIG. 4: Raman spectra of NREL *a*-Si film H14 compared to the U. Illinois *a*-Si film grown at 400 °C.

show that different CRN models can produce substantially different spectral density properties at low frequencies. Not surprisingly, we find that for the three CRNs compared in Figure 5 the peak sharpness increases with increasing structural order. The BM model has the highest structural order and EDIP has the lowest. For example, the BM model, which has the sharpest peaks, also has the lowest energy structure [9].

The Kubo based theory expresses κ_{Kubo} as an autorrelation function of an energy current operator S. In practice, due to discreteness in normal mode frequencies as a result of finite size of the models, the theory relies on an extrapolation of an applied frequency (Ω) dependent κ to $\Omega = 0$. Finite κ at small Ω comes from a non-zero overlap quantity, $\langle i|S_x|j\rangle$, involving the dynamical matrix, equilibrium positions, and pairs of normal mode eigenvectors $|i\rangle$ of nearby frequencies [7]. κ_{Kubo} can be written as

$$\kappa_{xx}(\Omega T) = \frac{\pi}{VT}\sum_{i,j}\frac{n_j - n_i}{\hbar\omega_{ij}}\left|\langle i|S_x|j\rangle\right|^2\delta_\eta(\omega_{ij}-\Omega), \tag{1}$$

where n_i represents the Bose occupation, ω_{ij} is a normal mode frequency difference $\omega_i - \omega_j$, and δ_eta is a Lorentzian of broadening parameter η [7]. The numerical results given here average κ_{ii} for $i = x, y, z$.

The computational results for the three models are shown in Figure 1, where $\eta = 0.022$ meV is chosen for all three models. Although we see a clear dependence of κ_{Kubo} on the structural ordering of the models, the values of κ_{Kubo} are smaller than any of the experimental results, even smaller than that of the TDTR at 9.8 MHz. Similar results have been interpreted in the past as due to contributions from low frequency modes omitted

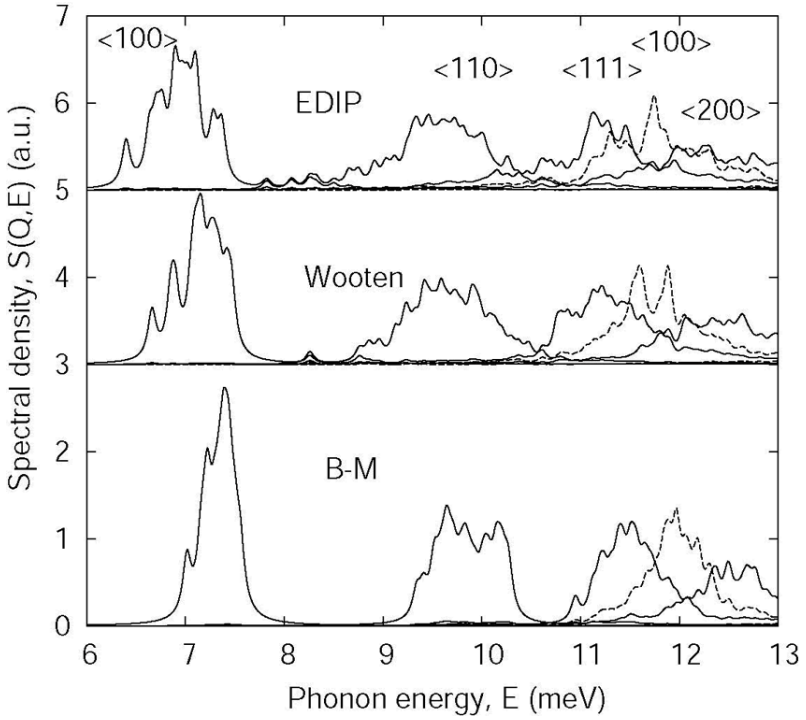

FIG. 5: $S(Q, E)$ for eigenvectors projected onto transverse (solid) and longitudinal (dashed) directions for the three CRNs. Sets of $\mathbf{Q}$ corresponding to each peak are indicated in units of $2\pi/L$, where $L = 27.26$ Åis the length of the computational cell.

from finite size of the models. It is necessary to augment the total κ with low frequency contributions κ_L, i.e., $\kappa = \kappa_{Kubo} + \kappa$. We consider approaches adopted by Cahill [13] for thin films and by Feldman [7] for thicker films, where boundary and TS scattering respectively was assumed to play a significant role. We then employed a quartic, i.e., Rayleigh, phonon scattering rate that was fit at the lower frequency limit of the computational model to the mode diffusivity, and used a Boltzmann transport theory that includes boundary scattering [22] and anharmonic scattering (estimated from numerical studies on crystalline silicon [23]). No TS scattering was included in this estimate because of the above-mentioned characteristics of the sample. With this model, which admittedly is most appropriate for a lateral steady state measurement, we can obtain κ to match our experimental results with a large `l` that is inconsistent with the film thicknesses and the nature of our experiments. The only physical model that we are aware of that yields larger κ, yet still an amorphous-like T dependence, is a nanocrystalline model [24], which is not applicable here. Instead, many experiments show that a judicious incorporation of a small amount H is the key for the superior material properties of this HWCVD sample [8]. Therefore, a well ordered a-Si:H model that incorporates right amount of H [25], or even a paracrystalline a-Si:H model [26], may be needed to achieve a better description of our results.

The dependence of the thermal conductivity on the frequency of the temperature

fields used in the measurements shown in Figure 2 suggests that a significant fraction of heat is carried by phonons with mean-free-paths that are comparable to thermal penetration depth. To extract quantitative information from these data requires a model for how the phonon lifetimes vary with frequency. For glasses and amorphous semiconductors at low frequencies, inverse quadratic or quartic dependencies are most often considered [27, 28]. The former can arise from either elastic scattering in the few meV region of the spectrum or from anharmonicity in the much lower frequency part. The latter is also often assumed as it represents Rayleigh scattering, although it yields a divergent result for an infinite harmonic solid.

If we assume that the frequency dependent TDTR results in Figure 2 correspond to κ from phonons with $\mathtt{l}$ less than the spatial extent of the thermal gradients, we can extract a simple scattering law appropriate to our experiment. We find that a scattering rate of ω^4 best represents the thin films (H14 and H35), while ω^2 the thicker film (H84) shown as dashed lines in Figure 2. It is important to remark that unless one believes that the thermal conductivity has reached a saturation value at the lowest modulation frequency of the experiment the temperature dependence as shown is deceptive, because within our theoretical model, the higher values of thermal conductivity for the lower temperature arise solely from the difference in thermal penetration depth between $T = 300$ K and $T = 115$ K at a fixed modulation frequency.

V. CONCLUSIONS

Amorphous Si prepared by HWCVD at the NREL shows a large enhancement in thermal conductivity compared to the prediction of the model of the minimum thermal conductivity. The magnitude, temperature, and frequency dependence of the conductivity more closely resembles the behavior of crystalline semiconductor alloys than the typical behavior of amorphous solids. We have not been able to reproduce this behavior, however, in *a*-Si prepared at the U. of Illinois by nominally the same growth technique although their Raman spectra look similar. Apparently, the anomalously high thermal conductivity of the NREL *a*-Si samples is produced by a unique microstructure that differs in a significant way from other *a*-Si where the model of the minimum thermal conductivity and the Kubo based theory seems to work well. This is consistent with the many other novel properties this amorphous material has manifested in prior studies, results which indicate that the NREL *a*-Si is much more ordered than other *a*-Si.

Acknowledgments

This research was supported by the U.S. Department of Energy grant No. DEFG02-91-ER45439 and the office of Naval Research.

References

* Electronic address: xiao.liu@nrl.navy.mil

[1] R. O. Pohl, X. Liu, and E. Thompson, Rev. Mod. Phys. **74**, 991 (2002).

[2] J. J. Freeman and A. C. Anderson, Phys. Rev. B **34**, 5684 (1986).

[3] V. Lubchenko and P. G. Wolynes, Proc. Natl. Acad. Sci. U.S.A. **100**, 1515 (2003).

[4] G. A. Slack, in *Solid State Physics: Advances in Research and Applications*, edited by H. Ehrenreich *et al.* (Academic, New York, 1979), Vol. 34, p. 1.

[5] David G. Cahill, S. K. Watson, and R. O. Pohl, Phys. Rev. B **46**, 6131 (1992).

[6] S. Alexander, O. Entin-Wohlman, and R. Orbach, Phys. Rev. B **34**, 2726 (1986).

[7] P. B. Allen and J. L. Feldman, Phys. Rev. Lett. **62**, 645 (1989); Phys. Rev. B **48**, 12581 (1993); J. L. Feldman, M. D. Kluge, P. B. Allen, and F. Wooten, Phys. Rev. B **48**, 12589 (1993).

[8] X. Liu, B. E. White Jr., R. O. Pohl, E. Iwanizcko, K. M. Jones, A. H. Mahan, B. N. Nelson, R. S. Crandall, and S. Veprek, Phys. Rev. Lett. **78**, 4418 (1997); X. Liu and R. O. Pohl, Phys. Rev. B **58**, 9067 (1998).

[9] J. L. Feldman, N. Bernstein, D. A. Papaconstantopoulos, and M. J. Mehl, J. Phys. Condens. Matter **16**, S5165 (2004).

[10] Y. K. Koh and D. G. Cahill, Phys. Rev. B **76**, 075207 (2007).

[11] D. G. Cahill, H. E. Fisher, T. Klitsner, and E. T. Swartz, J. Vac. Sci. Technol. A **7**, 1259 (1989).

[12] G. Pompe and E. Hegenbarth, Phys. Status Solidi B **147**, 103 (1988).

[13] D. G. Cahill, M. Katiyar, and J. R. Abelson, Phys. Rev. B **50**, 6077 (1994).

[14] L. Wieczorek, H. J. Goldsmid, and G. L. Paul, in *Thermal Conductivity 20*, edited by D. P. H. Hasselman and J. R. Thomas (Plenum, New York, 1989), p. 235.

[15] B. L. Zink, R. Pietri, and F. Hellman, Phys. Rev. Lett. **96**, 055902 (2006).

[16] B. S. W. Kuo, J. C. M. Li, and A. W. Schmid, Appl. Phys. A **55**, 289 (1992); L. Wei, M. Vaudin, C. S. Hwang, G. White, J. Xu, and A. J. Steckl, J. Mater. Res. **10**, 1889 (1995).

[17] S. T. Huxtable, A. R. Abramson, C-L. Tien, A. Majumdar, C. LaBounty, X. Fan, G. Zeng, J. E. Bowers, A. Shakouri, and E. T. Croke, Appl. Phys. Lett. **80**, 1737 (2002).

[18] H. M. Brodsky, M. Cardona, and J. J. Cuomo, Phys. Rev. B **16**, 3556 (1977).

[19] R. E. Cohen, M. J. Mehl, and D. A. Papaconstantopoulos, Phys. Rev. B **50**, 14 694 (1994); M. J. Mehl and D. A. Papaconstantopoulos, ibid. **54**, 4519 (1996).

[20] N. Bernstein, M. J. Mehl, D. A. Papaconstantopoulos, N. I. Papanicolaou, N. I. Bazant, and E. Kaxiras, Phys. Rev. B **62**, 4477 (2000); **65**, 249902 (2002).

[21] Y. H. Lee, R. Biswas, C. M. Soukoulis, C. Z. Wang, C. T. Chan, and K. M. Ho, Phys. Rev. B **43**, 6573 (1991).

[22] E. Ziambaras and P. Hyldgaard, J. Appl. Phys. **99**, 054303 (2006).

[23] A. Balandin and K. L. Wang, Phys. Rev. B **58**, 1544 (1998).

[24] A. Bodapati, P. K. Schelling, S. R. Phillpot, and P. Keblinski, Phys. Rev. B **74**, 245207 (2006).

[25] P. Biswas, R. Atta-Fynn, and D. A. Drabold, Phys. Rev. B **76**, 125210 (2007).

[26] P. M. Voyles, N. Zotov, S. M. Nakhmanson, D. A. Drabold, J. M. Gibson, M. M. J. Treacy, and P. Keblinski, J. Appl. Phys. **90**, 4437 (2001).

[27] C. Masciovecchio, G. Baldi, P. Benassi, S. Caponi, L. Comez, S. Di Fonzo, D. Fioretto, A. Fontana, A. Gessini, S. C. Santucci, F. Sette, G. Viliani, P. Vilmercati, and G. Ruocco, Phys. Rev. Lett. **97**, 035501 (2006).

[28] G. Baldi, P. Benassi, L. E. Bove, S. Caponi, E. Fabiani, D. Fioretto, A. Fontana, A. Giugni, M. Nardone, M. Sampoli, and F. Scarponi, Europhys. Lett. **78**, 36001 (2007).